Sensors and Materials, Vol. 8, No. 6 (1996) 317–326
MYU Tokyo

S & M 0248

A High-Performance Infrared Detector Using MOS Technology

Tadigadapa A. S. Srinivas, Paul J. Timans[1] and Haroon Ahmed

Microelectronics Research Center, Cavendish Laboratory,
University of Cambridge,
Madingley Road, Cambridge CB3 0HE, United Kingdom
[1]AG Associates, 4425 Fortran Drive, San Jose,
California 95134-2300, U.S.A.

(Received March 29, 1995; accepted December 11, 1995)

Key words: infrared detector, microthermopile, free-standing structure

This paper describes a free-standing microthermopile infrared detector. The device consists of micron-sized copper-constantan free-standing wires which overlap to form the hot junctions of the thermocouples, while the cold junctions are made from larger metal strips which are attached to the substrate. Incident radiation absorbed by the device causes the temperature of the free-standing hot junction to rise relative to the cold junction thereby resulting in a thermovoltage. These detectors were found to exhibit a response time of ~10 μs. The spectral response of the detectors was found to be 3 times higher at a wavelength of 10 μm compared to that at 1 μm and this difference is thought to be due to antenna effects. The antenna behavior of free-standing microthermocouples has been studied and the results from these experiments are also presented. The device is fabricated using standard silicon microfabrication techniques and can be integrated with active electronic circuits to result in a smart sensor.

1. Introduction

The ability to fabricate free-standing microstructures with small thermal masses and good thermal isolation using silicon micromachining technology has led to the development of miniaturized sensitive thermal infrared detectors.[1,2] The traditional approach has been to fabricate free-standing ~1-μm-thick membranes or cantilevers from dielectric layers of silicon nitride and silicon dioxide. The active structure for transducing the

infrared power into electrical signals is then fabricated onto these membranes and cantilevers.[3–5] An alternative approach is to do away with the supporting membrane altogether and directly fabricate free-standing structures from the active materials. Since the thermal isolation of these free-standing structures is better than that of membrane-based devices, direct use of them is expected to result in performance improvement of the devices. However, the limitation of this technique is that only materials with sufficiently strong mechanical properties, which can be fabricated as self-supporting free-standing structures, can be used. Based on this idea, a copper-constantan free-standing microthermocouple infrared detector was fabricated and has been reported earlier.[6,7] This paper was presented at the Europhysics Industrial Workshop 10 in Oberhof, Germany along with reports on some of the aspects of a free-standing microthermopile infrared detector.

Free-standing copper-constantan microthermocouples and microthermopiles have been fabricated and their thermal and infrared characteristics have been analyzed.[8] A typical microthermocouple is shown in Fig. 1 and consists of a 1-μm-wide and 20-μm-long free-standing wire, one half of which is copper and the other half is constantan. The hot junction is in the middle of the wire where the copper and constantan wires overlap, whereas the much larger cold junction is physically and thermally attached to the substrate. Absorption of the incident radiation by the device causes the hot junction to heat up relative to the cold junction and therefore produces a thermovoltage. The device has been fabricated on a 1000-Å-thick silicon nitride layer on silicon substrate using the "lift-off" process and isotropic $CF_4 + 8\%O_2$ plasma etching of the substrate.[6] Figure 2 shows a SEM micrograph

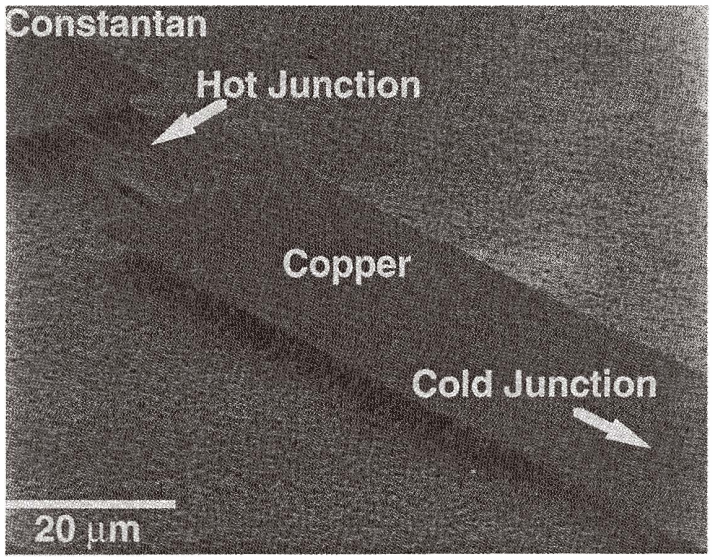

Fig. 1. SEM micrograph of a 1-μm-wide, 0.1-μm-thick and 20-μm-long free-standing microthermocouple. The hot junction is formed at the middle of the free-standing wire where the copper and constantan wires overlap.

of a microthermopile consisting of 20 thermocouples connected in series. In this case, a U-shaped copper free-standing structure was chosen for reasons of mechanical robustness and to accommodate lithographic misalignments during its fabrication. Since the device is fabricated using standard MOS microfabrication techniques, it should be possible to monolithically integrate the sensor with active circuits to result in a smart sensor.

2. Experimental Results

Responsivity, time constant and the spectral response of the microthermopiles described above have been measured in the 1–12 μm wavelength range. In an experiment reported earlier the time constant of the device was measured using an acoustooptic modulator in conjunction with a CO_2 laser.[7] The response of the microthermopile to a radiation step was measured and the time constant, τ_c, defined as the time taken by the output signal to rise to $(1 - e^{-1})$ or 63% of the peak value was found to be ~11 μs.[9] An alternative definition of τ_c is given by[10]

$$\tau_c = \frac{1}{2\pi f_{3db}} \tag{1}$$

where f_{3db} is the modulation frequency at which the output is 3 db below the steady state

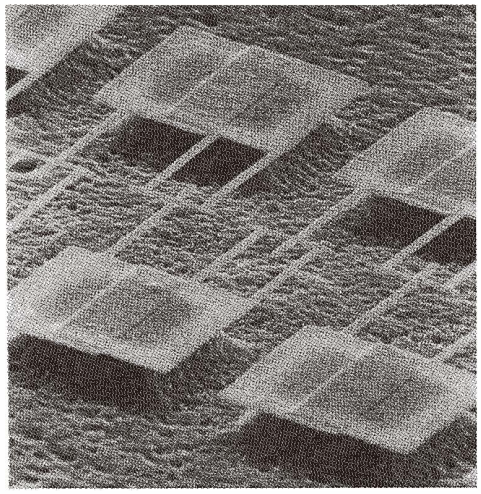

Fig. 2. SEM micrograph of a copper-constantan free-standing microthermopile. The cold junctions are the overlapping large pads; the hot junctions are formed at the intersection of the free-standing wires. The U-shaped free-standing structures are made of copper and the single wires are of constantan.

value, i.e., the voltage is 0.707 of the steady state voltage. In order to employ this definition of τ_c, the output of the detector was monitored as the CO_2 laser beam was sinusoidally modulated. This was achieved by sinusoidally modulating the laser cavity length using a piezoelectric drive in the grating mount. Keeping the peak-to-peak incident infrared power constant, the modulation frequency was varied from 100 Hz to 80 kHz. The detector output was monitored as a function of the modulation frequency and is shown in Fig. 3. At a frequency of 40 kHz the output is approximately 3 db below the output at 2 kHz and, using eq. (1), this implies τ_c of ~4 μs. Since f_{3db} has not been accurately measured, the error is expected to be large and explains the discrepancy in the τ_c's obtained by the two methods.

The responsivity of the microthermopile at 10.6 μm measured using a CO_2 laser was found to be 12.3 V/W.[9] In another experiment a 1.3-μm-wavelength buried-heterostructure laser was used to calibrate the detector. The laser gave a continuous output of 4 mW when operated at 25 mA over the threshold current. In order to determine the incident power density, a sharp blade edge was scanned across the laser to determine its beam profile. Figure 4 shows the microthermopile output as a function of incident power density from which the reponsivity of the device was deduced to be 3.4 V/W. The area of the detector was taken to be the cross-sectional area of the free-standing wires with respect to the incident beam which, for the device described here, is 1.1×10^{-9} m^2. The reponsivity of the

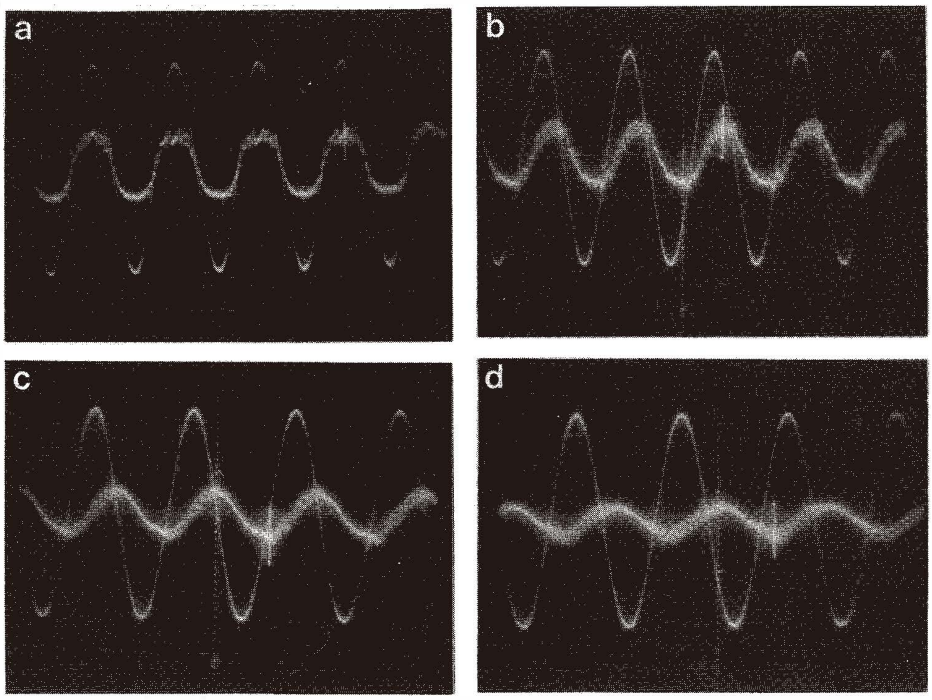

Fig. 3. Microthermopile output in response to an incident CO_2 laser beam which was modulated sinusoidally at the frequencies: (a) 2 kHz, (b) 20 kHz, (c) 40 kHz and (d) 80 kHz.

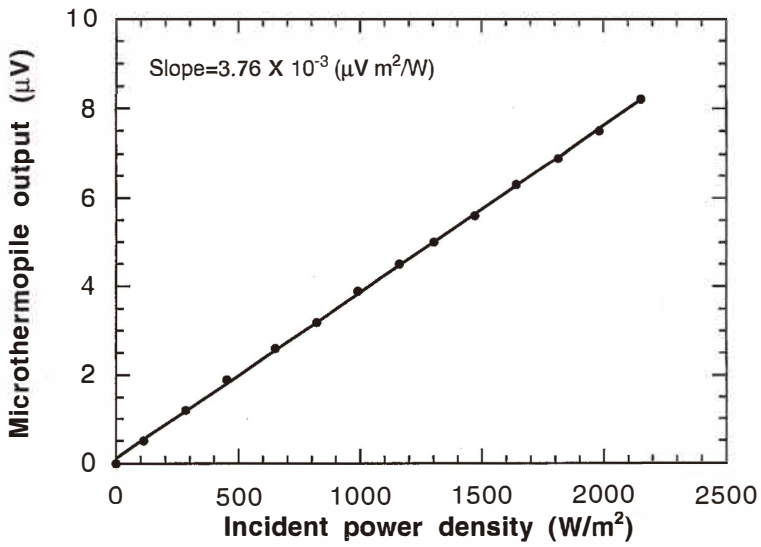

Fig. 4. Output of a free-standing microthermopile as a function of the incident laser power density at a wavelength of 1.3 μm. Dividing the slope of the curve by the detector area, i.e., the total surface area of the free-standing wires, which is 1.1×10^{-9} m^2, a responsivity of 3.4 V/W is obtained.

detector at 1.3 μm wavelength is about 3 times smaller than that at 10.6 μm. Such a behavior was also observed in the wavelength dependence of the relative response in the 1–12 μm wavelength range.[7] The reason for the rise in the relative response is not exactly understood but is thought to be due to the antenna effects arising from the interaction of the infrared radiation with the free-standing structures of the microthermopile. In order to study these antenna effects, microthermocouples of three different free-standing wire lengths of 20 μm, 40 μm and 60 μm and width 1 μm were fabricated and the results of the investigation are presented in the next section.

3. Analysis of a Free-Standing Microthermocouple as an Infrared Antenna

Infrared radiation incident on the free-standing metal structures induces electric currents in them at infrared frequencies. These electric currents are dissipated in the free-standing wire structures, causing them to heat up. The efficiency of this "transduction process" determines the responsivity of the device. Since the physical dimensions of the free-standing structures are smaller than or comparable to the wavelength of the radiation being detected, the problem of the interaction of the electromagnetic fields with the free-standing structures has been treated using the techniques of antenna theory. The structure

of the free-standing wire is analyzed as a transmitting antenna since, by the reciprocity theorem in antenna theory,[11] the conclusions remain unaffected when its role is reversed to that of a receiving antenna.

For the purposes of analysis, the free-standing wire forming the microthermocouple hot junction, Fig. 1, is assumed to be a dipole antenna, aligned along the z-axis of a right-handed Cartesian coordinate system with the hot junction at $z = 0$. The wires of copper and constantan forming the free-standing structure are assumed to be the two legs of a transmitting dipole antenna and the hot junction is replaced by a narrow gap across which the infrared signal is fed. The wider strip of metal leading to the cold junction, Fig. 1, is approximated by four wires tracing the perimeter of the metal strip. The assumption of the gap Δ to be infinitesimally small can be justified in this case, since $\Delta/\lambda = 1\ \mu\text{m}/10\ \mu\text{m} = 0.1 < 1$.

Infrared planar antennas fabricated on substrates exhibit properties different from those of antennas at lower frequencies.[12–14] In the infrared, metals are characterized by their surface impedance. The surface impedance of metals at infrared frequencies is much higher than at microwave frequencies because of the skin effect. This causes losses and damps the antenna currents, thereby degrading antenna performance. If τ denotes the relaxation time of the electrons in the metal, then at infrared frequencies $\omega\tau \gg 1$ and in this case the surface impedance Z_s is given by[15]

$$Z_s = \frac{1}{2}\sqrt{\frac{\mu_0\rho_0}{\tau}} + j\omega\sqrt{\mu_0\rho_0}\,, \tag{2}$$

where ω is the frequency, μ_0 is the permeability of free space, and ρ_0 is the dc resistivity of the metal. It can be seen from eq. (2) that, in the infrared, the resistive part of Z_s is a constant, but the reactance increases as the first power of the frequency. Thus at infrared frequencies the reactance is much more important than the resistance. Using the measured values of dc resistivities for the thin films of copper and constantan[9] and the value for the relaxation time of 2.7×10^{-14} s for Cu,[16] the surface impedances for copper and constantan can be calculated to be

$$Z_s\ (\text{copper}) = (1.6 + j\ 15.5)\ \Omega, \tag{3}$$

$$Z_s\ (\text{constantan}) = (3.5 + j\ 33.7)\ \Omega. \tag{4}$$

From the surface impedance, the loss impedance of any wire structure can be calculated using the expression[11]

$$Z_L = Z_s \frac{L}{2\pi a} \tag{5}$$

where Z_L is the loss impedance for the given wire structure, L is the length of the wire and a is its radius.

Since the wire forming the hot junction of the microthermocouple is free-standing, in

this simple analysis, the wire is assumed to be surrounded by free space and the effects of the substrate on the far field patterns have not been considered. The far field radiation pattern was computed for the three lengths $L = 20$ μm, 40 μm and 60 μm of the free-standing wires using a software package AWAS (Analysis of Wire Antennas and Scatterers).[17] AWAS is based on the two-potential equation for the distribution of antenna current. This integro-differential equation is solved numerically, using the method of moments with a polynomial (power series) approximation for the current distribution. Far field patterns have been evaluated considering the structure as a transmitting antenna. The antenna is assumed to be driven by a voltage source of frequency 28.3 THz, corresponding to a wavelength of 10.6 μm. A lumped impedance of magnitude equal to that of the impedance of the hot junction has been assumed across the input terminals of the source. A distributed impedance along the copper and constantan wire lengths of magnitude equal to the loss impedance was also assumed. The antenna dimensions in the model have been very closely approximated to those of the fabricated devices and the value of the far-zone electric field as a function of the azimuth angle θ was computed. The wire for $z > 0$ was assumed to be of copper while for $z < 0$ the wire was assumed to be made of constantan.

In order to experimentally investigate the microthermocouple output as a function of the angle θ, an x-z translation mount was fixed on a precision rotation stage with a least count of 1 minute of arc. The orientation of the microthermocouple in the socket was such that the rotations about the mounting post corresponded to variations in the angle θ. The experimental arrangement is schematically shown in Fig. 5. In practice, it was very difficult to mount the free-standing microthermocouple precisely on the axis of rotation of the optical mount. Thus, for every rotation, the device was found to have moved out of the line of the incident infrared beam and had to be corrected by translating it back into the laser beam. This was done by maximizing the output of the device for each angle by using the x-z translation micrometer screws. An error of ~ 5% was estimated in the process of maximization, due to the difficulty in aligning a 1-μm-wide free-standing wire to the exact maximum of the Gaussian intensity profile of an infrared laser—the experimental condition which would result in a maximum output. The output was measured at intervals of 5° from normal incidence. The experimental arrangement permitted a maximum rotation of 50°. Another limitation of the experimental arrangement was that the measurements had to be performed at an angle $\phi \sim 15°$, where ϕ is the angle from the normal to the wire surface in the plane perpendicular to the wire. The experimental results and the theoretical behavior of the free-standing structure as a function of θ, for $\phi = 15°$ and for the three different lengths of the free-standing wires, are plotted in Fig. 6. The error bars have been calculated as the standard deviation of four different measurements made at each angle.

Agreement between the predictions of the model and the experiments is not perfect but a number of features may be noted. There are striking periodicities in the measured outputs and these are mimicked quite well by the antenna calculation, particularly for the 20 and 60 μm devices as shown in Figs. 6(a) and 6(c), if a small translation of 2 – 4° is allowed in the patterns. Agreement for the 40 μm device is not as good although the peak at $\theta = 100°$ is predicted. The experimental setup has several limitations which include: the uncertainty in the exact orientation of the wire structure, the difficulty in signal maximization and the allowed maximum angular scan. Given the experimental constraints and the simplicity of the antenna modelling, the comparisons are quite encouraging. They are certainly good

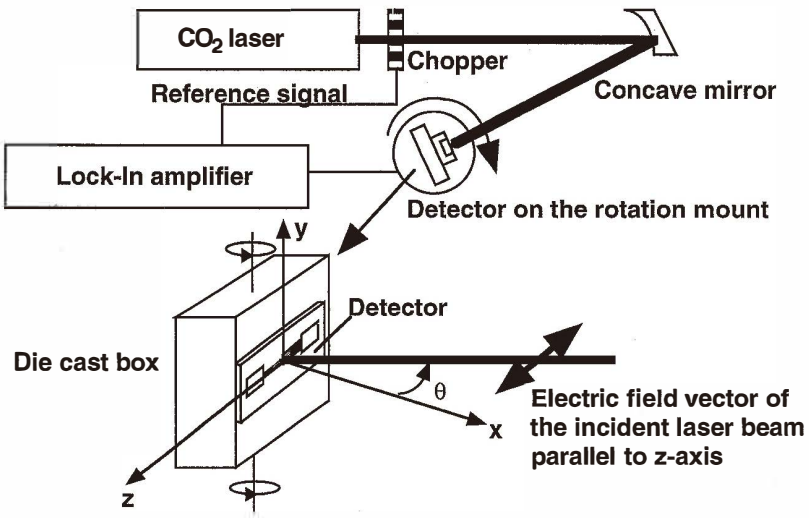

Fig. 5. Schematic diagram showing the experimental arrangement used for the measurement of the detector output as a function of the angle of incidence θ. Also illustrated is the relative orientation of the free-standing wire with respect to the incident electric field vector of the laser beam. Rotations about the mounting post correspond to variation in the angle θ.

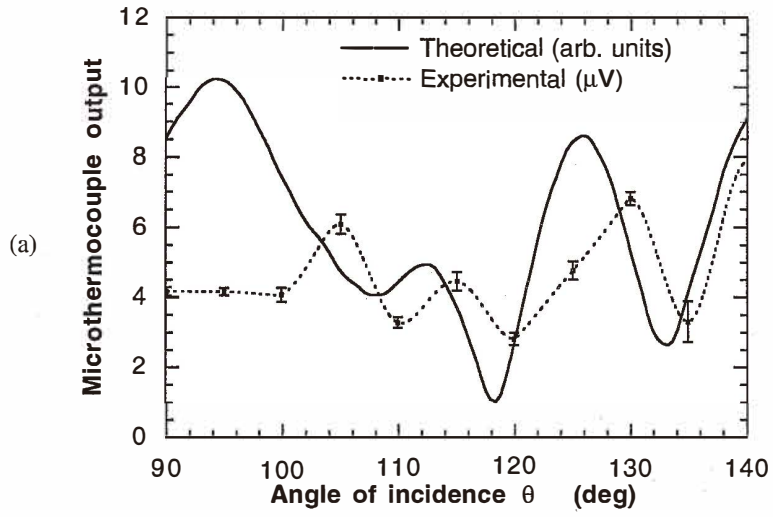

Fig. 6. Dependence of the output for (a) 20-μm-, (b) 40-μm- and (c) 60-μm-long free-standing wire microthermocouples on the angle of incidence θ. Also plotted is the variation of the signal output predicted using a simple model. Both the measurements and the calculations have been performed for $\phi = 15°$.

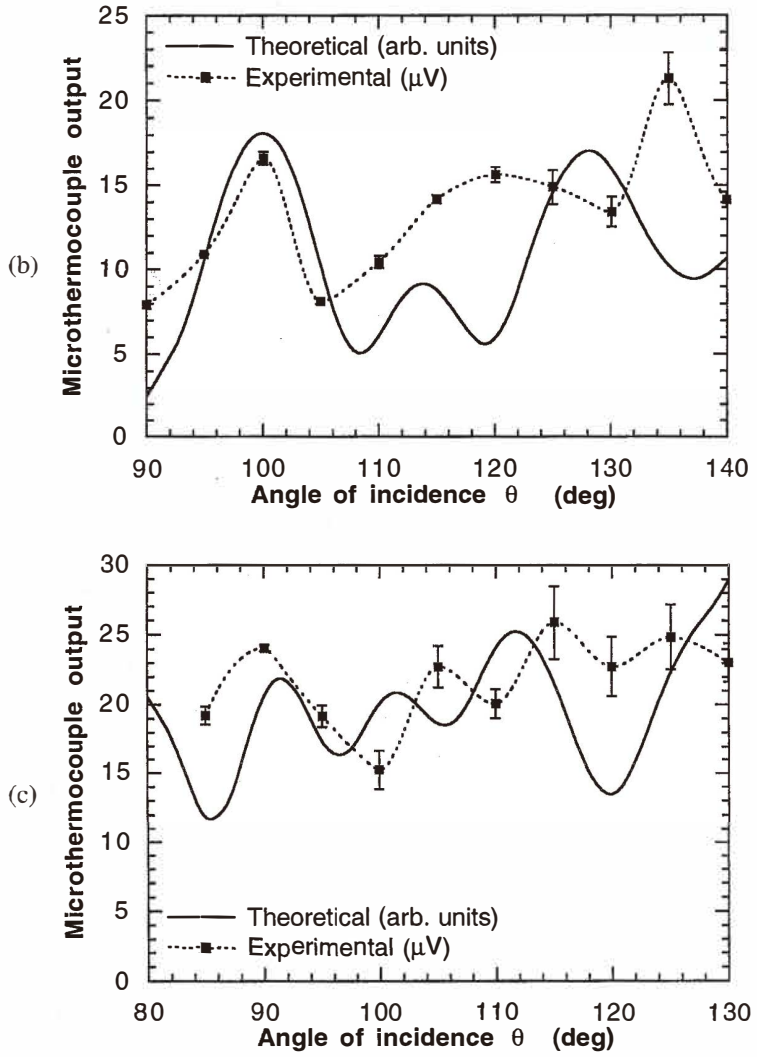

Fig. 6. (b) and (c).

enough to conclude that the devices are behaving as antennas at 10 μm. A more exact theoretical model should take the presence of the silicon substrate under the free-standing wires into consideration. In other experiments, the output of the microthermocouples was also found to be a function of the polarization of the incident radiation, which has already been reported.[8]

4. Conclusions

Free-standing microthermocouples and microthermopiles made from copper and constantan exhibit characteristics which are desirable for detecting infrared radiation and for CO_2 laser power measurements. The free-standing microthermopile infrared detector was found to be very fast with τ_c ~10 μs. The interaction of infrared radiation with the free-standing wires has been investigated using antenna theory. It should be possible to tailor the antenna properties exhibited by these devices to result in a high directional sensitivity of the output. Staring arrays consisting of these directional detectors can be employed, without the use of conventional optics, in infrared imagers and beam profilers. Besides power measurements, these detectors can also be used for the simultaneous determination of the polarization of CO_2 and other infrared lasers, which is of immense significance in spectroscopic and industrial applications of these lasers.

Acknowledgments

The authors would like to thank Dr. R. Padman for the use of AWAS software and Dr. R. J. Butcher for the use of the CO_2 laser.

References

1 H. Baltes: Physica Scripta **T49** (1993) 449.
2 R. A. Wood and N. A. Foss: Laser Focus World **29** (1993) 101.
3 G. R. Lahiji and K. D. Wise: IEEE Trans. Electron Devices **ED-29** (1982) 14.
4 F. Völklein, A. Wiegand and V. Baier: Sensors and Actuators **A 29** (1991) 87.
5 R. Lenggenhager, H. Baltes and T. Elbel: Sensors and Actuators **A 37–38** (1993) 216.
6 T. A. S. Srinivas, P. J. Timans, R. J. Butcher and H. Ahmed: Appl. Phys. Lett. **59** (1991) 1529.
7 T. A. S. Srinivas, P. J. Timans, R. J. Butcher and H. Ahmed: Sensors and Actuators **A 32** (1992) 403.
8 T. A. S. Srinivas, P. J. Timans, R. J. Butcher and H. Ahmed: Rev. Sci. Instrum. **64** (1993) 3602.
9 T. A. S. Srinivas: Ph. D. Thesis (Cambridge University 1992).
10 P. W. Kruse: The Photon Detection Process in Optical and Infrared Detectors, Topics in Applied Physics **19**, ed. R. J. Keyes (Springer, Berlin, 1977).
11 K. F. Lee: Principles of Antenna Theory (John Wiley, Chichester, 1984).
12 C. R. Brewitt-Taylor, D. J. Gunton and H. D. Rees: Electronics Lett. **17** (1981) 729.
13 T. Hwang, S. E. Schwarz and D. B. Rutledge: Appl. Phys. Lett. **34** (1979) 9.
14 N. Alexopoulos, P. B. Katehi and D. B. Rutledge: IEEE Trans. Microwave Theory and Techniques **MTT-31** (1983) 550.
15 D. B. Rutledge, S. E. Schwarz and A. T. Adams: Infrared Phys. **18** (1978) 713.
16 N. W. Ashcroft and N. D. Mermin: Solid State Physics (Holt, Rinehart and Winston, New York 1976).
17 AWAS (Analysis of Wire Antennas and Scatterers): Software and Users Manual, (Artech House, Boston, 1990).